NeuroImage: Clinical 24 (2019) 101971

Contents lists available at ScienceDirect

NeuroImage: Clinical

journal homepage: www.elsevier.com/locate/ynicl

Transcutaneous auricular vagus nerve stimulation at 1 Hz modulates locus coeruleus activity and resting state functional connectivity in patients with migraine: An fMRI study

Yue Zhang[a,1], Jiao Liu[b,c,1], Hui Li[d], Zhaoxian Yan[a], Xian Liu[a], Jin Cao[b], Joel Park[b], Georgia Wilson[b], Bo Liu[a,*], Jian Kong[b,*]

[a] Department of Radiology, The Second Affiliated Hospital of Guangzhou University of Chinese Medicine, Guangzhou 510120, China
[b] Department of Psychiatry, Massachusetts General Hospital, Harvard Medical School, 120 2nd Ave, Room 101, Charlestown, MA 02129, USA
[c] National-Local Joint Engineering Research Center of Rehabilitation Medicine Technology, Fujian University of Traditional Chinese Medicine, Fuzhou, Fujian 350122, China
[d] Department of Neurology, Guangdong Provincial Hospital of Chinese Medicine, Guangzhou 510120, China

ARTICLE INFO

Keywords:
Transcutaneous auricular vagus nerve stimulation
Locus coeruleus
Resting state functional connectivity
Migraine

ABSTRACT

Background: Migraine is a common episodic neurological disorder. Literature has shown that transcutaneous auricular vagus nerve stimulation (taVNS) at 1 Hz can significantly relieve migraine symptoms. However, its underlying mechanism remains unclear. This study aims to investigate the neural pathways associated with taVNS treatment of migraine.

Methods: Twenty-nine patients with migraine were recruited from outpatient neurology clinics. Each patient attended two magnetic resonance imaging/functional magnetic resonance imaging (MRI/fMRI) scan sessions separated by one week. Each session included a pre-stimulation resting state fMRI scan, fMRI scans during real or sham 1 Hz taVNS (with block design), and a post-stimulation resting state fMRI scan.

Results: Twenty-six patients were included in the final analyses. Real taVNS evoked fMRI signal decreases in brain areas belonging to the default mode network (DMN) and brain stem areas including the locus coeruleus (LC), raphe nuclei, parabrachial nucleus, and solitary nucleus. Sham taVNS evoked fMRI signal decreases in brain areas belonging to the DMN. Compared to sham taVNS, real taVNS produced greater deactivation at the bilateral LC. Resting state functional connectivity (rsFC) analysis showed that after taVNS, LC rsFC with the right temporoparietal junction and left secondary somatosensory cortex (S2) significantly increased compared to sham taVNS. The increased rsFC of the left LC-left S2 was significantly negatively associated with the frequency of migraine attacks during the preceding month.

Conclusion: Our results suggest that taVNS at 1 Hz can significantly modulate activity/connectivity of brain regions associated with the vagus nerve central pathway and pain modulation system, which may shed light on the neural mechanisms underlying taVNS treatment of migraine.

1. Introduction

The vagus nerve consists of a complex network that regulates pain, mood, the neuro-endocrine-immune axis, and memory (Kong et al., 2018; Yuan and Silberstein, 2016). Accumulating evidence suggests that transcutaneous vagus nerve stimulation may have the potential to relieve symptoms of migraine. In a previous study, Straube et al. (Straube et al., 2015) found that although both 1 Hz and 25 Hz transcutaneous auricular vagus nerve stimulation (taVNS) could produce symptom reduction in patients with migraine, those who received 1 Hz

Abbreviations: taVNS, transcutaneous auricular vagus nerve stimulation; MRI/fMRI, magnetic resonance imaging/functional magnetic resonance imaging; DMN, default mode network; LC, locus coeruleus; rsFC, resting state functional connectivity; S2, secondary somatosensory cortex; PBN, parabrachial nucleus; RN, raphe nuclei; ACC, anterior cingulate cortex; SN, solitary nucleus; ROIs, regions of interest; PCC, posterior cingulate cortex; mPFC, medial prefrontal gyrus; TPJ, temporoparietal junction

* Corresponding authors.
E-mail addresses: lbgdhtcm@163.com (B. Liu), kongj@nmr.mgh.harvard.edu (J. Kong).
[1] Yue Zhang and Jiao Liu are co-first authors.

https://doi.org/10.1016/j.nicl.2019.101971
Received 13 May 2019; Received in revised form 22 July 2019; Accepted 3 August 2019
Available online 05 August 2019

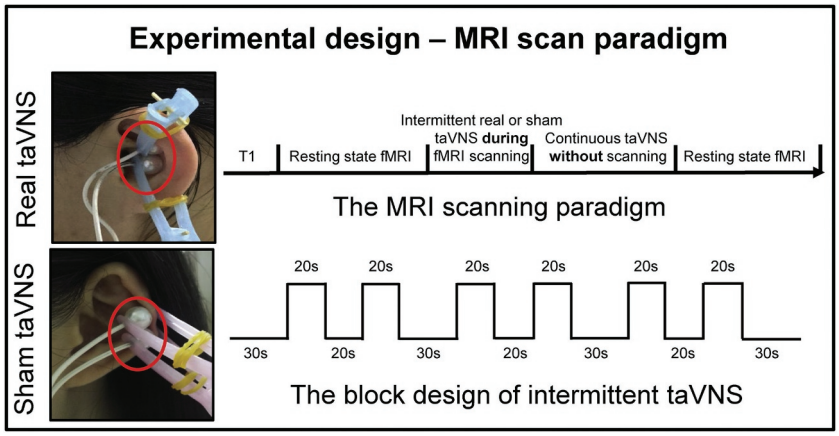

Fig. 1. Design of the study.

taVNS had a significantly larger reduction in headache days than patients who received 25 Hz after three months of treatment, highlighting the potential of 1 Hz taVNS for the treatment of migraine. However, the underlying mechanism of 1 Hz taVNS remains unclear.

Studies have suggested that the vagus nerve enters the nucleus tractus solitarius of the central nervous system and projects to the locus coeruleus (LC), parabrachial nucleus (PBN), and raphe nuclei (RN) of the brain stem and then ascends to higher brain regions such as the hippocampus, amygdala, anterior cingulate cortex (ACC), and hypothalamus (Beekwilder and Beems, 2010). A recent neuroimaging study (Fang et al., 2014) found that, compared with a control condition, taVNS at different frequencies can modulate the activity/connectivity of "classic" central vagal projections. For instance, Kraus et al. found thattaVNS at 8 Hz in the left outer auditory canal in healthy subjects significantly decreased the blood oxygen level dependence signal in limbic brain areas such as the amygdala, hippocampus, and para-hippocampal gyrus, and increased activation of the insula, precentral gyrus, and thalamus (Kraus et al., 2007).

To date, few studies have explored the brain response evoked by taVNS in patient populations. In a previous study, we found that taVNS at 20 Hz can produce an fMRI signal increase in the anterior insula and the increase can predict the one-month treatment response in patients with depression (Fang et al., 2017). In addition, we found that continuous taVNS at 20 Hz can significantly modulate the rsFC of the hypothalamus (Tu et al., 2018). In the only taVNS fMRI study with migraine, Garcia et al. investigated brain response to respiratory-gated taVNS at 30 Hz on episodic migraine patients and found that taVNS can modulate brain stem activity in the solitary nucleus and brain response to air-puff stimulation (Garcia et al., 2017). However, the central effect of 1 Hz taVNS, which produced significant symptom relief in patients with migraine (Straube et al., 2015) remains unknown.

In this study, we investigated the brain response to 1 Hz taVNS, as well as resting state functional connectivity (rsFC) changes after taVNS in patients with migraine in the interictal period as compared to sham taVNS. We hypothesized that taVNS may produce brain activity changes through the vagus nerve pathway and modulate the functional connectivity of brain networks associated with chronic pain.

2. Patients and methods

2.1. Patients

Twenty-nine patients with migraine were recruited in the present study from outpatient neurology clinics of the Second Affiliated Hospital of Guangzhou University of Chinese Medicine. Informed consent was obtained from all participants. This study protocol was approved by the Institutional Review Board of the Second Affiliated Hospital of Guangzhou University of Chinese Medicine.

Episodic migraineurs without aura were recruited for this study. Similar to our previous study (Li et al., 2017), the diagnosis of migraine was based on the International Classification of Headache Disorders, 2nd Edition (ICHD-II), as diagnosed by a specialist working at the neurology outpatient service of the Second Affiliated Hospital of Guangzhou University of Chinese Medicine. The inclusion criteria were as follows: 1. Aged 18–45 years old; 2. Right-handed; 3. At least six months of migraine duration; 4. Have at least two headache attacks per month; 5. Have not taken any prophylactic headache medications during the past one month; 6. Have not taken any psychoactive or vasoactive drugs during the past three months.

Participants were excluded from the study if any of the following criteria were met: 1. Headache induced by other diseases; 2. Headache attack within 48 h prior to the experiment or during the experiment; 3. Pregnant or lactating; 4. Any other chronic pain conditions; 5. Severe head deformity or intracranial lesions; 6. Score on the Self-Rating Anxiety Scale (SAS) or Self-Rating Depression Scale (SDS) >50.

2.2. Experimental design

A single-blind, crossover fMRI trial design was applied in the present study to investigate the immediate modulation effects of real and sham taVNS. Specifically, each patient attended two MRI scanning visits with identical parameters that were separated by at least one week, one for real taVNS and another for sham taVNS. This crossover design has two advantages compared to a parallel randomized study. First, the influence of confounding covariates is reduced because each crossover patient serves as their own control, and second, crossover designs are statistically efficient and have more power to test hypotheses.

In the present study, we applied auricular vagus nerve electrical stimulation at the left cymba concha (the real stimulation site) (Badran et al., 2018). The control (sham) stimulation site was on the left tail of the helix (Fig. 1). We chose these stimulation sites because a previous study reported that the cymba conchae of the ear contains the highest density of auricular vagus nerve projections (100%), while the tail of the helix of the ear is free of cutaneous vagal innervation (Peuker and Filler, 2002). Previous studies also suggested that electrical stimulation of vagal projections in the ear, such as the cymba conchae, inner side of the tragus, and outer auditory canal, can produce stronger fMRI signal modulation compared to regions of the ear without vagal innervation, such as the top of the helix (Kraus et al., 2013; Yakunina et al., 2017).

The stimulation was applied with the MRI compatible Electronic Acupuncture Treatment Instrument (SDZII, Huatuo, Suzhou, China) with a continuous wave (frequency: 1 Hz; width: 0.2 ms). Stimulation intensity was adjusted to approximately 1.5–3 mA, the strongest

sensation indviduals can tolerate without pain.

All magnetic resonance imaging/functional magnetic resonance imaging (MRI/fMRI) scanning was conducted on a 3.0T Siemens MRI scanner (Siemens MAGNETOM Verio 3.0 T, Erlangen, Germany) with a 24-channel phased-array head coil. Subjects were told to stay awake, remain motionless, and keep their eyes closed during the scan. Each scanning session lasted approximately 30 min. The order of MRI scans was: a high-resolution anatomical image (MPRAGE), an eight-minute resting state functional MRI scan, a five-minute real or sham taVNS fMRI scan (block design), eight minutes of continuous real or sham taVNS (fMRI was not applied during this continuous stimulation period), and another eight-minute resting state functional MRI scan (Fig. 1).

MPRAGE was applied with the following parameters: TR = 1900 ms, TE = 2.27 ms, flip angle = 9°, FOV = 256 mm × 256 mm, matrix = 256 × 256, and slice thickness = 1.0 mm. The resting state functional MRI was acquired with the following parameters: TR = 2000 ms, TE = 30 ms, FOV = 224 mm × 224 mm, matrix = 64 × 64, flip angle = 90°, slice thickness = 3.5 mm, interslice gap = 0.7 mm, 31 axial slices paralleled and 240 time points. The real and sham taVNS scans were collected using echoplanar imaging sequences in a block design. The scanning parameters were: TR = 2000 ms, TE = 30 ms, FOV = 224 mm × 224 mm, matrix = 64 × 64, slice thickness = 3.5 mm, 31 slices and phases = 150. Each scan consisted of six 20-s "on" conditions separated by 20- or 30-s "off" periods (Fig. 1).

Disease duration, frequency of migraine attacks during the past month, score on the visual analog scale (VAS) before the first MRI scan, and score on the Migraine Specific Quality-of-Life Questionnaire (MSQ) within the ten minutes preceding the first fMRI scan were measured.

3. Data processing and analysis

3.1. Real and sham taVNS fMRI data analysis

Real and sham taVNS fMRI data processing and analysis were performed with SPM12 (https://www.fil.ion.ucl.ac.uk/spm/software/spm12/) using MATLAB. The first three timepoints were deleted before data preprocessing. The data preprocessing was conducted as follows: slice-timing of functional data to correct for timing differences between slices; realignment to reduce motion-related variance; co-registration of functional and anatomical data and segmentation (grey matter, white matter, and cerebrospinal fluid); spatial normalization to the Montreal Neurological Institute space and smoothing with a 6-mm full width half maximum (FWHM).

At the subject level, the contrast between real/sham taVNS vs. no stimulation was calculated using a general linear model. Group analyses were performed using a random-effects model. A one-sample *t*-test was performed to compare fMRI signal changes during real or sham taVNS vs. no stimulation within each treatment condition. A threshold of voxel-wise $p < .001$ uncorrected and cluster-level $p < .05$ False Discovery Rate (FDR) corrected was applied. A paired t-test was used to compare fMRI signal change differences between real and sham taVNS at a threshold of voxel-wise $p < .005$ uncorrected and cluster-level $p < .05$ FDR corrected.

Since the solitary nucleus (SN) and locus coeruleus (LC) are important nodes in the VNS pathway (Busch et al., 2013), we pre-defined the bilateral LC and SN as regions of interest (ROIs) in the contrast between real and sham taVNS. The bilateral LC was defined according to Bär (Bär et al., 2016) (combined left and right LC; left LC was defined as 4 × 6 × 10 mm centered at MNI-coordinates −5, −34, −21, and right LC was defined as 4 × 6 × 10 mm centered at MNI-coordinates 7, −34, −21). The bilateral SN (combinate left and right, sphere radius = 12 mm, MNI-coordinates: ±2, −46, −60) was defined following a study conducted by Frangos and Komisaruk (2017). Similar to our previous study (Liu et al., 2019a, 2019b), a threshold of voxel-wise $p < .005$ was used in ROI data analysis. Monte Carlo simulations using 3dFWHMx and 3dClustSim [AFNI (https://afni.nimh.nih.gov/) released in July 2017] were applied to correct for multiple comparisons.

To investigate the association between the evoked fMRI signal change (between real and sham taVNS) and the clinical outcomes (frequency of migraine attack, disease duration, VAS, MSQ scores), we extracted mean beta values of the brain regions that had a significant group difference between real and sham taVNS. We then performed a multiple regression analysis between the mean beta values change (real taVNS minus sham taVNS) and the clinical outcomes (frequency of migraine attack, disease duration, VAS, MSQ scores) across all subjects after Bonferroni correction.

3.2. Seed-to-voxel resting state functional connectivity analysis

The seed-to-voxel correlational analysis was applied with CONN toolbox v17.C (http://www.nitrc.org/projects/conn) (Liu et al., 2019a, 2019b; Tao et al., 2019; Tao et al., 2016). The bilateral LC, which was evoked by the taVNS (21 voxels, real < sham, see the Results section and Table 2 for details), was used as the region of interest.

The preprocessing of images included slice-timing correction, realignment, co-registration to subjects' respective structural images, normalization, and smoothing with a 4-mm FWHM kernel. To remove the temporal confounding factors, segmentation of grey matter, white matter, and cerebrospinal fluid areas was employed. A frequency window of 0.01 to 0.089 Hz was used for band-pass filtering.

To eliminate correlations caused by head motion and artifacts, we identified outlier time points in the motion parameters and global signal intensity using ART (https://www.nitrc.org/projects/artifact_detect). Similar to our previous study (Tao et al., 2016), images whose composite movement exceeded 0.5 mm or whose global mean intensity was greater than three standard deviations from the mean image intensity were treated as outliers. The temporal time series of the head motion matrix of outliers was also entered as first-level covariates.

In the first-level analysis, we produced a correlation map for each subject by extracting the BOLD time course from the LC seed and computing Pearson's correlation coefficients between the time course in the bilateral LC and every voxel of the whole brain. Seed-to-voxel between-group connectivity analyses were performed using a paired *t*-test (real vs. sham, post-stimulation minus pre-stimulation). A threshold of voxel-wise $p < .005$ uncorrected and cluster-level $p < .05$ FDR corrected were applied for comparison between real and sham taVNS.

Given the important role of the ACC, amygdala, and hypothalamus in the pathophysiology of migraine (Brennan and Pietrobon, 2018) and the descending pain modulation system (Li et al., 2016; Millan, 2002), we pre-defined the bilateral amygdala and bilateral ACC as regions of interest (ROIs) using the AAL brain atlas and bilateral hypothalamus from the TD Bradman brain atlas using WFU_Pick_Atlas toolbox. A threshold of voxel-wise $p < .005$ was used in data analysis. To correct for multiple comparisons, Monte Carlo simulations using the 3dFWHMx and 3dClustSim [AFNI (https://afni.nimh.nih.gov) released in July 2017] were applied.

To investigate the association between rsFC change and clinical outcomes (frequency of migraine attack, disease duration, VAS, MSQ scores), we extracted the average z values of the brain regions that had significant rsFC with the LC after taVNS. We then performed a multiple regression analysis between the rsFC z value change and the clinical outcomes (frequency of migraine attack, disease duration, VAS, MSQ scores) across all subjects after Bonferroni correction.

4. Results

Twenty-nine patients with migraine were recruited. Among those, one patient refused to participate in the MRI scan, and one subject diagnosed with a cerebral lacunar infarction and another with an arachnoid cyst were withdrawn. Twenty-six (four male and twenty-two female) patients completed the study and were included in data analysis

Table 1
Patient demographics (n = 26).

Characteristics	
Gender (male/female)	4/22
Age (mean ± SD)	32.50 ± 7.57
Disease duration in years (mean ± SD)	7.15 ± 2.87
Frequency per month (mean ± SD)	3.23 ± 1.58
VAS (mean ± SD)	51.03 ± 11.88
MSQ (mean ± SD)	59.00 ± 9.18
SDS score (mean ± SD)	40.50 ± 5.17
SAS score (mean ± SD)	40.31 ± 3.91

VAS, Visual Analog Scale; MSQ, Migraine Specific Quality-of-Life Questionnaire; SDS, Self-rating Depression Scale; SAS, Self-rating Anxiety Scale.
Frequency: the frequency of migraine attacks during the past month.
VAS measures the average attack intensity of the four weeks preceding the first fMRI scanning.
The MSQ, SDS, and SAS were administered within the ten minutes preceding the first fMRI scanning.

(Table 1).

Patients' characterization of disease duration and score on VAS, MSQ, SDS, SAS measured before the first MRI scan are shown in Table 1. No patient reported administration of acute migraine medications or having an attack 48 h prior to or following the MRI sessions.

4.1. fMRI signal changes evoked by real and sham taVNS

4.1.1. Real and sham taVNS stimulation results

A whole-brain one sample t-test showed that real taVNS produced significant fMRI signal increases in the bilateral putamen, right caudate, right pallidum/anterior insula, right thalamus, and left frontal operculum (Table 2, Supplementary Fig. 1A) and widespread fMRI signal decreases in the bilateral precuneus/posterior cingulate cortex (PCC)/hippocampus/precentral gyrus/medial prefrontal gyrus (mPFC)/anterior cingulate cortex (ACC), bilateral LC, left SN, right RN/PBN, left posterior insula, and bilateral superior/middle frontal gyrus during real taVNS compared to baseline (Table 2, Fig. 2 A1 and A2, Supplementary Fig. 1B).

There was no significant fMRI signal increase at the threshold we set (voxel-wise $p < .001$ uncorrected and cluster-level $p < .05$ FDR corrected) during sham taVNS. However, we detected significantly widespread fMRI signal decreases in the bilateral mPFC/ACC/caudate, bilateral precentral gyrus/postcentral gyrus/precuneus/middle occipital gyrus, left inferior temporal gyrus/bilateral hippocampus/fusiform gyrus/lingual gyrus, left middle/superior frontal gyrus, left inferior occipital gyrus, right occipital fusiform gyrus, left middle frontal gyrus, left middle temporal gyrus, right temporal pole, left posterior insula, and right middle/superior frontal gyrus during sham taVNS compared to baseline (Table 2 and Supplementary Fig. 1C).

A direct comparison between real and sham taVNS showed that there was no significant fMRI signal difference for whole-brain analysis at the threshold we set. ROI analysis detected significantly more deactivation in the bilateral LC (k = 8) in real taVNS compared to sham taVNS (Table 2, Fig. 2 A3).

We extracted mean beta values of the bilateral LCthat had significant group differences between real and sham taVNS and performed a multiple regression analysis between the mean beta values change (real taVNS minus sham taVNS) and clinical outcomes (frequency of migraine attack, disease duration, VAS, MSQ scores) across all subjects. We did not find any significant associations after Bonferroni correction (0.05/4).

4.2. Resting state functional connectivity results

Seed-to-voxel whole-brain rsFC analysis using the LC as a seed showed significantly increased rsFC in the right temporoparietal junction (TPJ), right para-hippocampus/hippocampus, right superior temporal gyrus, and left central operculum/secondary somatosensory cortex (S2) following real taVNS compared to sham taVNS.

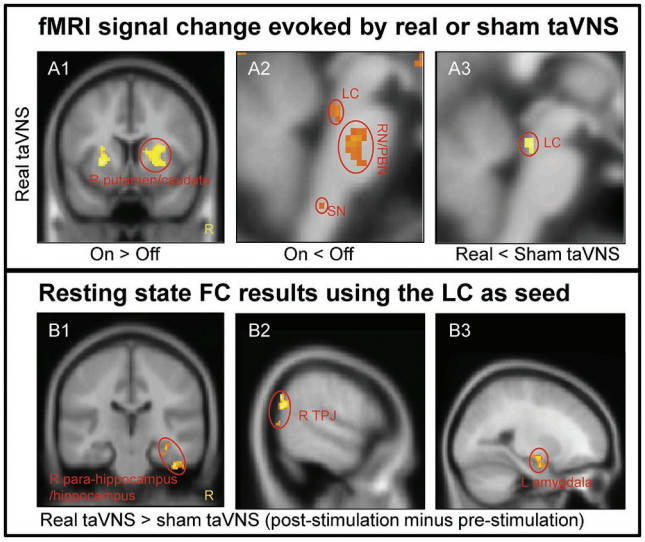

Fig. 2. The results of fMRI data analysis. A. fMRI results evoked by taVNS. A1. Increased brain activation in the real taVNS group; A2. Decreased brain activation in the real taVNS group. A3. Group difference in brain region activation between real and sham taVNS during stimulation. B. Resting state functional connectivity results using the LC as seed. B1. Increased rsFC in the right para-hippocampus/hippocampus in real taVNS compared to sham taVNS; B2. Increased rsFC in the right TPJ in real taVNS compared to sham taVNS; B3. Increased rsFC in the left amygdala in real taVNS compared to sham taVNS (LC: locus coeruleus; RN: raphe nuclei; PBN: parabrachial nucleus; SN: solitary nucleus; TPJ: temporoparietal junction; R: right).

ROI analysis showed significantly increased LC rsFC in the left amygdala (k = 20) during real taVNS compared to sham taVNS at the threshold we set (Table 3, Fig. 2B1–B3).

In addition, we extracted the average z values of all five brain regions (Table 3),that had significant rsFC with the LC after taVNS (Table 3) and assessed their association with clinical outcomes (frequency of migraine attack, disease duration, VAS, MSQ scores). We found a significant negative association between the rsFC z value change at the left S2 and the frequency of migraine attacks in the preceding month ($p = .002$, $r = -0.58$), and a significant positive association between disease duration and rsFC z value change at the right TPJ (p = .002, $r = 0.57$) across all subjects after Bonferroni correction (0.05/20)(Fig. 3A and B).

5. Discussion

In the present study, we investigated fMRI signal changes and resting state functional connectivity changes evoked by real and sham 1 Hz taVNS in migraineurs. We found that real taVNS produced fMRI signal increases at the insula, operculum, putamen, and caudate and MRI signal decreases in the brain areas belonging to the default mode network (DMN), bilateral LC, left SN, and right RN/PBN of the brainstem. Sham taVNS also produced deactivation in the brain areas belonging to the DMN. Compared to sham stimulation, real taVNS produced significant fMRI signal decreases at the LC. Using the LC as a seed, we found that real taVNS produced significant rsFC increases with the right TPJ, right para-hippocampus, left S2, and left amygdala compared to sham taVNS. The increased rsFC with the left S2 was significantly negatively associated with the frequency of migraine attacks during the preceding month. These findings suggest that taVNS at 1 Hz can significantly modulate brain regions associated with the vagus

Table 2
Change in fMRI signal evoked by real and sham taVNS and group difference between real and sham taVNS (mPFC: medial prefrontal cortex; PCC: posterior cingulate cortex; ACC: anterior cingulate cortex).

Contrast	Cluster	Brain region	Peak T value	Peak Z value	MNI coordinates		
					X	Y	Z
Real taVNS							
On > Off	506	Right putamen	5.99	4.67	28	0	−2
		Right pallidum	5.43	4.37	20	4	−2
		Right anterior insula	4.59	3.87	26	8	12
		Right caudate	4.29	3.68	18	2	16
		Right thalamus	4.17	3.60	4	−8	6
	201	Left putamen	5.46	4.39	−26	2	0
		Left frontal operculum	3.74	3.30	−6	12	12
On < Off	37,152	Bilateral precuneus	7.69	5.46	−6	−46	52
		Bilateral PCC	7.10	5.20	−8	−38	54
		Bilateral hippocampus	7.50	5.38	−30	−26	−12
		Bilateral precentral gyrus	7.10	5.20	−8	−38	54
		Bilateral mPFC	6.97	5.15	−8	38	−16
		Bilateral ACC	6.96	5.14	18	24	−12
	148	Bilateral locus coeruleus	4.28	3.67	−3	−34	−22
		Left solitary nucleus	4.20	3.62	−6	−46	−54
	132	Right raphe nucleus/parabrachial nucleus	5.34	4.32	10	−26	−30
	126	Left posterior insula	4.97	4.11	−32	−26	16
	162	Bilateral superior frontal gyrus	4.58	3.87	−20	40	40
		Bilateral middle frontal gyrus	4.02	3.50	−30	32	32
Sham taVNS							
On > Off	No brain region above the threshold						
On < Off	3203	Bilateral mPFC	7.90	5.55	−10	42	−12
		Bilateral ACC	6.41	4.88	−8	34	−12
		Bilateral caudate	6.33	4.85	−14	20	−6
	19,964	Bilateral precentral gyrus	7.29	5.29	−24	−24	68
		Bilateral postcentral gyrus	7.12	5.22	−20	−30	66
		Bilateral precuneus	5.95	4.65	6	−58	52
		Bilateral middle occipital gyrus	5.84	4.60	34	−78	38
	1166	Left inferior temporal gyrus	6.03	4.69	−46	−22	−26
		Bilateral hippocampus	5.91	4.63	−26	−36	−8
		Bilateral fusiform gyrus	5.65	4.49	−36	−16	−28
		Bilateral lingual gyrus	4.19	3.61	−16	−40	−10
	319	Left middle frontal gyrus	5.97	4.66	−26	38	32
		Left superior frontal gyrus	4.47	3.80	−26	30	46
	211	Left inferior occipital gyrus	5.97	4.66	−50	−70	−18
	348	Right hippocampus	5.73	4.54	26	−12	−20
		Right fusiform gyrus	4.45	3.79	34	−34	−28
	456	Right occipital fusiform gyrus	4.60	3.88	20	−86	−14
	175	Left middle frontal gyrus	5.56	4.44	−40	20	28
	102	Left middle temporal gyrus	5.27	4.28	−58	−18	−16
	114	Right temporal pole	4.87	4.04	48	14	−30
	152	Left posterior insula	4.66	3.92	−30	−26	18
	266	Right middle frontal gyrus	4.64	3.91	28	38	42
		Right superior frontal gyrus	4.38	3.73	24	28	44
Real taVNS vs *Sham taVNS*							
Real < Sham	21	Bilateral locus coeruleus	3.99	3.48	−2	−34	−20
Real > Sham	No brain region above the threshold						

Table 3
Resting state functional connectivity results using the LC as a seed.

Contrast (post-pre)	Cluster	Brain region	Peak T value	Peak Z value	MNI coordinates		
					X	Y	Z
Real > Sham	267	Right temporoparietal junction	6.60	4.98	56	−64	30
	187	Right para-hippocampus	4.05	3.52	32	−26	−20
		Right hippocampus	3.96	3.46	34	−24	−16
	180	Right superior temporal gyrus	4.28	3.67	48	−16	−8
	126	Left central operculum (S2)	3.77	3.32	−50	−8	6
	84	Left amygdala	4.25	3.65	−24	−6	−20
Real < Sham	No brain region above the threshold						

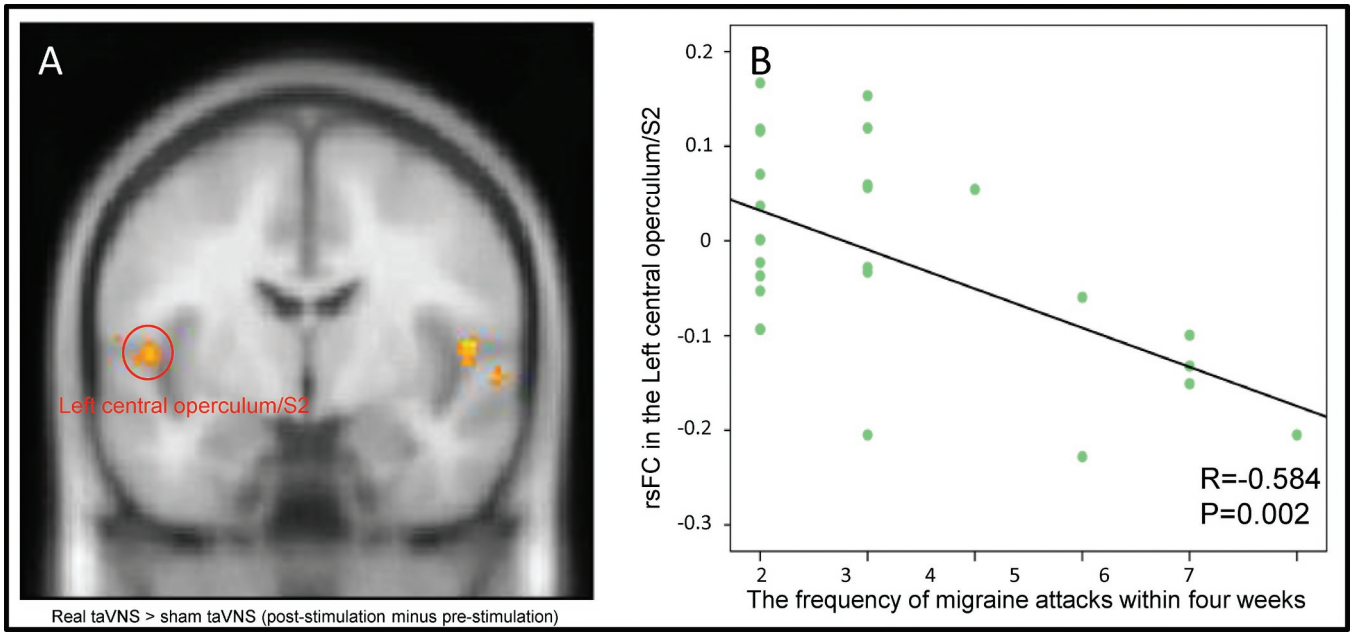

Fig. 3. The results of rsFC and frequency of migraine attacks during the preceding month. A. Increased rsFC in the left S2 and LC. B. The scatter plot shows the significant association between left S2-LC rsFC and the frequency of migraine attacks during the preceding month.

nerve central pathway and pain modulation system.

Our results showing that both real and sham taVNS produced an fMRI signal decrease in the brain areas belonging to the DMN is consistent with studies suggesting that the DMN is a deactivated brain network in specific attention-demanding or stimulus-dependent tasks (Raichle, 2015).

We also found that real 1 Hz taVNS significantly deactivates hubs of the vagus nerve pathway, such as the LC, RN, and PBN. Compared to sham taVNS, real taVNS produced a greater fMRI signal decrease at the LC. These results are consistent with previous studies in which investigators found that VNS can modulate fMRI signals at the LC in healthy subjects (Fang et al., 2014) and also in chronic tinnitus patients (Yakunina et al., 2018). Literature has suggested that stress is a common condition in migraine (Sauro and Becker, 2009) and norepinephrine (NE) may be involved in the neural process of migraine (Wei et al., 2015). The LC is a major node of norepinephrine release in the stress response and plays a key role in different pain conditions via the descending and ascending LC-spinal pathways (Llorca-Torralba et al., 2016). Mokha reported that the inhibitory action evoked by electrical stimulation in the LC plays a role in the modulation of analgesia (Mokha et al., 1986). We thus believe the modulation effect of taVNS on the LC may provide support for applying taVNS to relieve symptoms of migraine.

Compared to sham taVNS, real taVNS produced increases in LC rsFC with the right TPJ, left amygdala, hippocampus/para-hippocampus, and left S2. In addition, we also found a significant positive association between disease duration and the rsFC change at the right TPJ. The TPJ is a key brain region of the ventral frontoparietal network of attention. A study found that, compared to non-migraineurs, migraineurs showed less activation in the right TPJ during both voluntary and reflexive visual spatial orienting (Mickleborough et al., 2016).

The amygdala is a key region in the descending pain modulation system and has a direct connection with the periaqueductal grey (Chen and Heinricher, 2019). Our previous study found that chronic pain is associated with disrupted rsFC between the periaqueductal grey and the amygdala (Yu et al., 2014). In addition, we found that one month of taVNS can significantly modulate the rsFC of the amygdala in patients with depression (Liu et al., 2016), which is partly consistent with the findings of this study.

The hippocampus/para-hippocampus is a key region in the limbic system and plays an important role in memory encoding and retrieval. Recently, studies have suggested that structures of the limbic system, including the hippocampus/para-hippocampus and amygdala, play an important role in the pathophysiology of chronic pain and the modulation of chronic pain (Vachon-Presseau, 2018). The modulation of taVNS on the LC and limbic system further endorses its potential in the treatment of chronic pain.

We also found a significant increase in rsFC of LC-S2 in the real taVNS group. This rsFC between LC and S2 is associated with frequency of migraine attacks in the month preceding the experiment. More specifically, more increased rsFC of LC-S2 is correlated with fewer migraine attacks. We also found that after real taVNS, as compared to sham, LC-S2 functional connectivity significantly increased. These findings imply that taVNS may decrease the frequency of migraine attacks by modulating the rsFC of LC-S2. The S2 is one of the primary hubs of the pain matrix (Kong et al., 2010), and Orenius et al. suggested that it is also involved in the interaction of pain and emotion (Orenius et al., 2017). Taken together, our finding that taVNS modulates LC rsFC with the amygdala, hippocampus/para-hippocampus, and S2 in patients with migraine suggests that taVNS can significantly enhance the descending pain modulation system, cognition, and emotion regulation to relieve symptoms of migraine.

There are several limitations to our present study. First, stimulation frequency is a crucial parameter in taVNS. Investigators have used different frequencies in previous studies, and theoptimal frequency may vary for different disorders (Kong et al., 2018). In a randomized clinical trial, investigators found that although both 1 Hz and 25 Hz taVNS can produce clinical improvement, 1 Hz taVNS produced a greater treatment effect than 25 Hz taVNS (Straube et al., 2015). We thus focused on 1 Hz taVNS in this study. Further study is needed to investigate how different frequencies can influence brain activity and connectivity in patients with migraine. Second, a crossover design was used in the present study, in which each patient served as his/her own matched control. All MRI scans were performed when participants were not experiencing migraine, and we thus did not assess the acute treatment effect of real and sham taVNS. In addition, in the present study, we included patients who had not taken any prophylactic headache medication during the past month. However, several of these migraine

medications may have longer half-lives, and medications taken more than one month ago may still affect treatment outcomes. Nevertheless, we have used a crossover design, which may at least partially control for the potential residual effects of medications. Furthermore, this study was performed with migraine patients. Whether the activity/connectivity changes/patterns produced by taVNS in healthy subjects are the same in migraine patients remains unclear. Finally, patients in this study tended to have a relatively low migraine attack frequency. Future studies with larger sample sizes and larger ranges of migraine attack frequency may be more representative.

6. Conclusion

We found that taVNS at 1 Hz can 1) produce a significant fMRI signal decrease at the LC and 2) increase rsFC between the LC and the TPJ, amygdala, hippocampus/para-hippocampus, and left S2 compared to sham taVNS. Our findings indicate that taVNS can modulate the vagus nerve pathway and pain modulation networks in patients with migraine, highlighting the potential for 1 Hz taVNS treatment of migraine.

Declaration of Competing Interest

JK has a disclosure to report (holding equity in a startup company, MNT, and pending patents to develop a new brain stimulation device) but declares no conflict of interest. All other authors declare no competing interests.

Acknowledgements

This study was supported by the Medical Scientific Research Foundation of Guangdong Province of China (A2017234) and the Administration of Traditional Chinese Medicine of Guangdong Province of China (20182047).

Author contributions

Experimental design: Bo Liu and Jian Kong; data collection: Yue Zhang, Hui Li, Zhaoxian Yan, Xian Liu; data analysis: Jiao Liu, Jin Cao; manuscript preparation: Jiao Liu, Jian Kong, Joel Park, Georgia Wilson, and Yue Zhang.

All authors contributed to manuscript preparation and have read and approved the final manuscript.

Supplementary material

Supplementary material associated with this article can be found, in the online version, at doi:10.1016/j.nicl.2019.101971.

References

Badran, B., Brown, J., Dowdle, L., Mithoefer, O., LaBate, N., Coatsworth, J., DeVries, W., Austelle, C., McTeague, L., Yu, A., Bikson, M., Jenkins, D., George, M., 2018. Tragus or cymba conchae? Investigating the anatomical foundation of transcutaneous auricular vagus nerve stimulation (taVNS). Brain Stimulation 11, 947–948. https://doi.org/10.1016/j.brs.2018.06.003.

Bär, K.J., De la Cruz, F., Schumann, A., Koehler, S., Sauer, H., Critchley, H., Wagner, G., 2016. Functional connectivity and network analysis of midbrain and brainstem nuclei. NeuroImage 134, 53–63. https://doi.org/10.1016/j.neuroimage.2016.03.071.

Beekwilder, J.P., Beems, T., 2010. Overview of the clinical applications of vagus nerve stimulation. J. Clin. Neurophysiol. 27, 130–138. https://doi.org/10.1097/WNP.0b013e3181d64d8a.

Brennan, K., Pietrobon, D., 2018. A systems neuroscience approach to migraine. Neuron 97, 1004–1021. https://doi.org/10.1016/j.neuron.2018.01.029.

Busch, V., Zeman, F., Heckel, A., Menne, F., Ellrich, J., Eichhammer, P., 2013. The effect of transcutaneous vagus nerve stimulation on pain perception-an experimental study. Brain Stimulation 6, 202–209. https://doi.org/10.1016/j.brs.2012.04.006.

Chen, Q., Heinricher, M., 2019. Descending control mechanisms and chronic pain. Curr. Rheumatol. Rep. 21, 13.

Fang, L., Hong, Y., Fan, Y., Liu, J., Ma, Y., Xiu, C., 2014. Brain response to transcutaneous electronical stimulation on auricular concha of the healthy subjects using fMRI. Chin. J. Magn. Reson. Imaging 5, 416–422.

Fang, J., Egorova, N., Rong, P., Liu, J., Hong, Y., Fan, Y., Wang, X., Wang, H., Yu, Y., Ma, Y., Xu, C., Li, S., Zhao, J., Luo, M., Zhu, B., Kong, J., 2017. Early cortical biomarkers of longitudinal transcutaneous vagus nerve stimulation treatment success in depression. NeuroImage: Clinical 14, 105–111. https://doi.org/10.1016/j.nicl.2016.12.016.

Frangos, E., Komisaruk, B.R., 2017. Access to Vagal Projections via Cutaneous Electrical Stimulation of the Neck: fMRI Evidence in Healthy Humans. Brain Stimulation 10, 19–27. https://doi.org/10.1016/j.brs.2016.10.008.

Garcia, R.G., Lin, R.L., Lee, J., Kim, J., Barbieri, R., Sclocco, R., Wasan, A.D., Edwards, R.R., Rosen, B.R., Hadjikhani, N., Napadow, V., 2017. Modulation of brainstem activity and connectivity by respiratory-gated auricular vagal afferent nerve stimulation in migraine patients. Pain 158, 1461–1472. https://doi.org/10.1097/j.pain.0000000000000930.

Kong, J., Loggia, M.L., Zyloney, C., Tu, P., LaViolette, P., Gollub, R.L., 2010. Exploring the brain in pain: activations, deactivations and their relation. Pain 148, 257–267. https://doi.org/10.1016/j.pain.2009.11.008.

Kong, J., Fang, J., Park, J., Li, S., Rong, P., 2018. Treating depression with transcutaneous auricular vagus nerve stimulation: state of the art and future perspectives. Front. Psychiatry 9, 20. https://doi.org/10.3389/fpsyt.2018.00020.

Kraus, T., Hösl, K., Kiess, O., Schanze, A., Kornhuber, J., Forster, C., 2007. BOLD fMRI deactivation of limbic and temporal brain structures and mood enhancing effect by transcutaneous vagus nerve stimulation. J. Neural Transm. 114, 1485–1493. https://doi.org/10.1007/s00702-007-0755-z.

Kraus, T., Kiess, O., Hösl, K., Terekhin, P., Kornhuber, J., Forster, C., 2013. CNS BOLD fMRI effects of sham-controlled transcutaneous electrical nerve stimulation in the left outer auditory canal - a pilot study. Brain Stimulation 6, 798–804. https://doi.org/10.1016/j.brs.2013.01.011.

Li, Z., Liu, M., Lan, L., Zeng, F., Makris, N., Liang, Y., Guo, T., Wu, F., Gao, Y., Dong, M., Yang, J., Li, Y., Gong, Q., Liang, F., Kong, J., 2016. Altered periaqueductal gray resting state functional connectivity in migraine and the modulation effect of treatment. Sci. Rep. 6, 20298. https://doi.org/10.1038/srep20298.

Li, Z., Fang, Z., Tao, Y., Lei, L., Nikos, M., Kristen, J., Taipin, G., 2017. Acupuncture modulates the abnormal brainstem activity in migraine without aura patients. NeuroImage: Clinical 15, 367–375.

Liu, J., Chen, L., Chen, X., Hu, K., Tu, Y., Lin, M., Huang, J., Liu, W., Wu, J., Qiu, Z., Zhu, J., Li, M., Park, J., Wilson, G., Lang, C., Xie, G., Tao, J., Kong, J., 2019. Modulation effects of different exercise modalities on the functional connectivity of the periaqueductal grey and ventral tegmental area in patients with knee osteoarthritis – a randomized multi-modal MRI study. British J. Anesthesia. https://doi.org/10.1016/j.bja.2019.06.017. (in press).

Liu, J., Fang, J., Wang, Z., Rong, P., Hong, Y., Fan, Y., Wang, X., Park, J., Jin, Y., Liu, C., Zhu, B., Kong, J., 2016. Transcutaneous vagus nerve stimulation modulates amygdala functional connectivity in patients with depression. J. Affect. Disord. 205, 319–326. https://doi.org/10.1016/j.jad.2016.08.003.

Liu, J., Tao, J., Liu, W., Huang, J., Xue, X., Li, M., Yang, M., Zhu, J., Lang, C., Park, J., Tu, Y., Wilson, G., Chen, L., Kong, J., 2019. Different modulation effects of Tai Chi Chuan and Baduanjin on resting state functional connectivity of the default mode network in older adults. Soc. Cogn. Affect. Neurosci. 14, 217–224. https://doi.org/10.1093/scan/nsz001.

Llorca-Torralba, M., Borges, G., Neto, F., Mico, J., Berrocoso, E., 2016. Noradrenergic locus Coeruleus pathways in pain modulation. Neuroscience 338, 93–113. https://doi.org/10.1016/j.neuroscience.2016.05.057.

Mickleborough, M.J.S., Ekstrand, C., Gould, L., Lorentz, E.J., Ellchuk, T., Babyn, P., Borowsky, R., 2016. Attentional network differences between Migraineurs and non-migraine controls: fMRI evidence. Brain Topogr. 29, 419–428. https://doi.org/10.1007/s10548-015-0459-x.

Millan, M., 2002. Descending control of pain. Prog. Neurobiol. 66, 355–474. https://doi.org/10.1016/S0301-0082(02)00009-6.

Mokha, S.S., McMillan, J.A., Iggo, A., 1986. Pathways mediating descending control of spinal nociceptive transmission from the nuclei locus coeruleus (LC) and raphe magnus (NRM) in the cat. Exp. Brain Res. 61, 597–606. https://doi.org/10.1007/BF00237586.

Orenius, T.I., Raij, T.T., Nuortimo, A., Näätänen, P., Lipsanen, J., Karlsson, H., 2017. The interaction of emotion and pain in the insula and secondary somatosensory cortex. Neuroscience 349, 185–194. https://doi.org/10.1016/j.neuroscience.2017.02.047.

Peuker, E.T., Filler, T.J., 2002. The nerve supply of the human auricle. Clin. Anat. 15, 35–37. https://doi.org/10.1002/ca.1089.

Raichle, M.E., 2015. The Brain's default mode network. Annu. Rev. Neurosci. 38, 433–447. https://doi.org/10.1146/annurev-neuro-071013-014030.

Sauro, K., Becker, W., 2009. The stress and migraine interaction. Headache 49, 1378–1386. https://doi.org/10.1111/j.1526-4610.2009.01486.x.

Straube, A., Ellrich, J., Eren, O., Blum, B., Ruscheweyh, R., 2015. Treatment of chronic migraine with transcutaneous stimulation of the auricular branch of the vagal nerve (auricular t-VNS): a randomized, monocentric clinical trial. J. Headache Pain 16, 63. https://doi.org/10.1186/s10194-015-0543-3.

Tao, J., Liu, J., Egorova, N., Chen, L., Sun, S., Xue, H., Huang, J., Zheng, H., Wang, Q., Chen, D., Kong, J., 2016. Increased hippocampus-medial prefrontal cortex resting-state functional connectivity and memory function after Tai Chi Chuan practice in elder adults. Front. Aging Neurosci. 8, 25. https://doi.org/10.3389/fnagi.2016.00025.

Tao, J., Liu, J., Chen, X., Xia, R., Li, M., Huang, M., Li, S., Park, J., Wilson, G., Lang, C., Xie, G., Zhang, B., Zheng, G., Chen, L., Kong, J., 2019. Mind-body exercise improves cognitive function in patients with mild cognitive impairment and centrally modulates the hippocampus/ACC: a multi-modal MRI study. NeuroImage: Clinical 23,

101834. https://doi.org/10.1016/j.nicl.2019.101834.
Tu, Y., Fang, J., Cao, J., Wang, Z., Park, J., Jorgenson, K., Lang, C., Liu, J., Zhang, G., Zhao, Y., Zhu, B., Rong, P., Kong, J., 2018. A distinct biomarker of continuous transcutaneous vagus nerve stimulation treatment in major depressive disorder. Brain Stimulation 11, 501–508. https://doi.org/10.1016/j.brs.2018.01.006.
Vachon-Presseau, E., 2018. Effects of stress on the corticolimbic system: implications for chronic pain. Prog. Neuro-Psychopharmacol. Biol. Psychiatry 20, 216–223. https://doi.org/10.1016/j.pnpbp.2017.10.014.
Wei, X., Yan, J., Tillu, D., Asiedu, M., Weinstein, N., Melemedjian, O., Price, T., Dussor, G., 2015. Meningeal norepinephrine produces headache behaviors in rats via actions both on dural afferents and fibroblasts. Cephalalgia 35, 1054–1064. https://doi.org/10.1177/0333102414566861.
Yakunina, N., Kim, S.S., Nam, E.C., 2017. Optimization of transcutaneous vagus nerve stimulation using functional MRI. Neuromodulation 20, 290–300. https://doi.org/10.1111/ner.12541.
Yakunina, N., Kim, S.S., Nam, E.C., 2018. BOLD fMRI effects of transcutaneous vagus nerve stimulation in patients with chronic tinnitus. PLoS One 13, e0207281. https://doi.org/10.1371/journal.pone.0207281.
Yu, R., Gollub, R.L., Spaeth, R., Napadow, V., Wasan, A., Kong, J., 2014. Disrupted functional connectivity of the periaqueductal gray in chronic low back pain. NeuroImage: Clinical 6, 100–108. https://doi.org/10.1016/j.nicl.2014.08.019.
Yuan, H., Silberstein, S.D., 2016. Vagus nerve and Vagus nerve stimulation, a comprehensive review: part I. Headache 56, 71–78. https://doi.org/10.1111/head.12647.